HOKKAIDO UNIVERSITY

Title	High-temperature properties of extruded titanium composites fabricated from carbon nanotubes coated titanium powder by spark plasma sintering and hot extrusion
Author(s)	Kondoh, Katsuyoshi; Threrujirapapong, Thotsaphon; Umeda, Junko; Fugetsu, Bunshi
Citation	Composites Science and Technology, 72(11), 1291-1297 https://doi.org/10.1016/j.compscitech.2012.05.002
Issue Date	2012-06-28
Doc URL	http://hdl.handle.net/2115/49691
Type	article (author version)
File Information	CST72-11_1291-1297.pdf

Instructions for use

High-temperature properties of extruded titanium composites fabricated from carbon nanotubes coated titanium powder by spark plasma sintering and hot extrusion

Katsuyoshi Kondoh[1] [*], Thotsaphon Threrujirapapong[2], Junko Umeda[1], Bunshi Fugetsu[3]

[1] Joining and Welding Research Institute, Osaka University, Osaka, Japan.

[2] Industrial Engineering Department, Naresuan University, Phitsanulok, Thailand.

[3] Graduate School of Environmental Science, Hokkaido University, Hokkaido, Japan

Abstract

Pure titanium matrix composite reinforced with carbon nanotubes (CNTs) was prepared by spark plasma sintering and hot extrusion via powder metallurgy process. Titanium (Ti) powders were coated with CNTs via a wet process using a zwitterionic surfactant solution containing 1.0, 2.0 and 3.0wt.% of CNTs. *In-situ* TiC formation via reaction of CNTs with titanium occurred during sintering, and TiC particles were uniformly dispersed in the matrix. As-extruded Ti/TiCs composite rods were annealed at 473 K for 3.6 ks to reduce the residual stress during processing. After annealing process, the tensile properties of the composites were evaluated at room temperature, 473, 573 and 673 K, respectively. Hardness test was also performed at room temperature up to 573 K with a step of 50 K. The mechanical properties of extruded Ti/CNTs composites at elevated temperature were remarkably improved by adding a small amount of CNTs, compared to extruded Ti matrix. These were due to the TiC dispersoids originated from CNTs effectively stabilized the microstructure of extruded Ti composites by their pinning effect. Moreover, the coarsening and growth of Ti grain never occurred even though they were annealed at 573, 673 K for 36 ks and 673 K for 360 ks, respectively.

Keywords

1. Introduction

Since the official report of carbon nanotubes (CNTs) by Iijima in 1991 [1], they have been expected to be a promising reinforcement in composite materials processing because they remarkably show superior mechanical properties such as high Young's modulus of about 1TPa and tensile strength of about 20 GPa [2-4]. Recently, CNTs have been widely used as reinforcing materials for metal matrix composites (MMCs). The previous studies indicated the remarkable characteristics of MMCs reinforced with CNTs, such as aluminium [5-7], magnesium [8-10], copper [11-12] and titanium [13-16]. Ti and its alloys are also interested as competitive matrix materials because they exhibit high specific strength which is an important factor for weight reduction of the airplane and automotive applications from the viewpoint of energy consumption. The previous work [14] has demonstrated a successful improvement of tensile properties at room temperature of the commercially pure Ti reinforced with CNTs via wet processing in powder metallurgy route. However, the improvement of mechanical properties of commercially pure Ti at elevated temperature is also important because some applications need to use or exposure to high temperature such as exhaust system of airplanes, automotives and power plants [17-18]. Xue et al. [16] have reported good compressive properties of Ti/CNTs composite materials at 873 K. However, the tensile properties and hardness of those Ti/CNTs composite materials at elevated temperature have not been studied. In the present study, the commercially pure titanium matrix reinforced with TiC particles and CNTs were prepared by wet processing, and consolidated by spark plasma sintering and hot extrusion as wrought composites. The effect of dispersoids in the Ti matrix on microstructures of the composites at elevated temperature was investigated. Finally, the tensile properties and hardness of extruded Ti/TiCs composites were evaluated at elevated temperature

2 Experimental

The pure Ti powders grade 2 with the purity of 95% were used as starting materials. The mean particles size of pure Ti powders is 30 μm. The chemical compositions of the pure Ti powders are listed in **Table 1**. Carbon nanotubes (CNTs) made by Bayer MaterialScience with an average diameter of 20 nm and 1~ 10 μm in length were used as the reinforcing materials in the present study. Typical linear zwitterionic surfactant solutions containing the CNTs concentration of 1.0, 2.0 and 3.0wt.% were prepared. The pure Ti powders were coated by the different concentration of the aqueous CNT/zwitterionic solutions and subsequently dried in an oven at 373 K for 10.8 ks. The solid zwitterionic substances were solidified as thin film solids and existed on the Ti surface during drying process. Those thin film solids needed to be eliminated before consolidation because they were changed to gases at temperature of above 773 K [14], resulting in pore defects in the consolidated bulk materials. The coated Ti powders were heated again in a horizontal tube furnace at 873 K for 3.6 ks under a protective Ar gas. The image of CNT coated Ti particle is shown in **Fig. 1**. The Ti powders coated with CNTs were consolidated by SPS (Syntech Co. SPS-103S) process at 1073 K for 1.8 ks under vacuum (<4Pa). The applied pressure during SPS process was constantly kept at 30 MPa. The sintered Ti billet was then heated to 1273 K for 180 s under an Ar atmosphere, and immediately underwent to a hot extrusion process. The extrusion ratio, speed, mold and die temperature were 37, 3.0 mm/s and 673 K, respectively.

To reduce the residue stress during processing, the extruded Ti composites were annealed at the low temperature of 473 K for 360 ks. The microstructure and phase characterization of extruded Ti composites were investigated by optical microscopy, a scanning electron microscope (SEM, JEOL: JSM-6500F) and X-ray diffractometer (XRD,

Shimadzu: XRD-6100). The Cohen's method of least square analysis [19] was used to estimate the change of lattice parameter, a and c axes, of the extruded Ti composite materials. Moreover, the amount of *in-situ* formed TiC dispersoids was also estimated by comparing the peak intensity ratio of TiC/Ti in the XRD results with a TiC calibration curve. The internal standard technique [19] was used to prepare the TiC calibration curve by plotting the ratio of maximum intensity of TiC/Ti peaks in XRD result against the known concentration of TiC particles in the Ti powders. The extruded Ti composites after the annealing process were machined into tensile specimen bars of 3.0 mm in diameter and 20 mm in gauge length. The tensile properties at room temperature were evaluated using universal test machine (Autograph AG-X 50kN, Shimadzu) under a strain rate of 5 $\times 10^{-4}$ s^{-1} Hardness at room temperature was also measured by a micro-Vickers hardness tester (Shimadzu: HMV-2T). In addition, the tensile properties at elevated temperature were evaluated using a horizontal high temperature tensile testing machine (Yonekura: CATY-T3H-KD 5KN) at 473, 573 and 673 K, respectively, under the same strain rate as mentioned above. Hardness at elevated temperatures was also evaluated by the same hardness tester which was attached to homemade heating equipment. The holding time at the given temperature before measurement of both tensile and hardness test was 300 s.

3. Results and discussion

Fig. 2 shows the optical microstructure images of extruded pure Ti material before and after annealing at 473 K for 360 ks. The grain size measurements before and after annealing of those extruded pure Ti material with no CNT indicate the average value of 11.7 and 44.7 μm, respectively. A large increase in grain size of extruded pure Ti material is due to the recovery process and coarsening of Ti grain occurred during a long time annealing [20]. On the other hand, the microstructures of extruded pure Ti/TiCs

composites both before and after annealing process reveal the unchanged grain size as shown by the representative microstructures of the extruded pure Ti/TiC by using 1.0wt.% CNTs/zwitterionic solution in **Fig.2**(c) and (d). The grain size measurement results of all composite materials almost show the same size in the range of 7.4 to 8.6 μm as summarized in **Table 2.** The very small changes in grain size are due to the pinning effect of TiC dispersiods which retard the Ti grain coarsening during annealing process as mentioned next.

XRD patterns of the extruded Ti composites after annealing are shown in **Fig. 3**. The XRD results have confirmed only *in-situ* formed TiC dispersoid, not TiO_2 and TiN, existing in the Ti matrix. That means no oxidation and nitridation were detected by XRD inside the extruded Ti/TiCs composites during SPS, hot extrusion and annealing process. A quantitative estimation of the *in-situ* formed TiC dispersoid content reveals the TiC contents of 0.61, 1.58 and 2.55 wt.% for the composite by using 1.0, 2.0 and 3.0 wt.% CNTs/zwitterionic solution, respectively. Furthermore, the lattice expansion of Ti matrix is also calculated to investigate the possibility of carbon atom dissolved into the Ti matrix. The calculation of precise lattice parameters, a and c, of Ti using the Cohen's least squares method [19] indicated that the carbon atom originating from CNTs and/or *in-situ* formed TiC dispersoids can be dissolved into Ti matrix, resulting in expansion of Ti lattice parameters. The amount of dissolved carbon atom can be further estimated by comparing the Ti lattice expansion results with the master plot which was reported by H. Conrad [21]. The calculation of Ti lattice parameters and the estimation results of the TiC dispersoid amount, dissolved carbon atom and the carbon content analysis are summarized in **Table 3**. It should be note that the maximum equilibrium solubility of carbon in α-Ti from is 0.4 wt.% [22]

The tensile test results at room temperature and elevated temperature of extruded Ti/TiCs composites after annealing at 473 K for 3.6 ks are shown in **Fig. 4**. The improvement of mechanical properties, in particular yield stress, of the composites at room temperature can be considered that due to the effect of grain size, solid solution of carbon and TiC second phase including the remained CNTs [10, 14]. The strengthening mechanism due to grain size effect was estimated by Hall-Petch relationship [23-24] using the material constants in Ref. [24]. The values of σ_0 and k constants are 172.5 MPa and 18 MPa √mm, respectively, at room temperature. Unfortunately, due to the lack of information of k constants for elevated temperatures, the estimation steps were started by comparing the yield stress in this study and the previous results [25] to obtain k constants, and then the rest constant will be obtained. The estimated values of σ_0 constants are 1.9, 2.7 and 2.0 MPa, and k constants are 17.5, 8.4 and 9.3 MPa √mm for the temperatures of 473, 573 and 673 K, respectively. It should be noted that the k constant of 17.5 MPa √mm at 473 is close to 18 MPa √mm [24] at room temperature. This can be implied that the strain hardening effect due to grain size is strongly dominated the yield stress of extruded pure Ti during tensile testing until 473 K. After 473 K, the k constant is obviously decreased because of the increasing effect of recovery process in accordance with the previous reports [25]. The effect of carbon solid solution can be estimated by comparing the amount of dissolved carbon atom in this study with a plot of the dependence of carbon solute atom on the incremental yield stress in the previous study [21]. The strengthening mechanisms of each effect are summarized in **Table 4**. As the results of strengthening estimation, the increase of yield stress of the extruded Ti/TiCs composites are mainly due to the dispersion strengthening mechanism of the second phases (TiC particles and the remained CNTs) and the grain size effect, while the carbon solid solution shows a very small effect on the increase of yield stress. The effects of oxygen and nitrogen [21, 26]

are also taken into account in the same effect as well as carbon. However, the previous study [27] suggested that the oxygen and nitrogen contents in the composite, which was consolidated using the same materials and conditions with this study, are very small and close to the starting content in the raw powders. Therefore, the effect of oxygen and nitrogen may not significantly increase the mechanical properties of extruded Ti composites at room temperature and elevated temperature, compared to the effect of *in-situ* formed TiC dispersoids in this study. The remained CNTs have been detected in the fractured surfaces of all samples after annealing process and tensile testing at elevated temperatures as shown by the representative sample of the extruded pure Ti/TiCs by using 1.0wt.% CNTs/zwitterionic solution tested at 673 K in Fig. 5. Unfortunately, the exact strengthening mechanism by the remained CNTs in the Ti composites at room and elevated temperatures is still unclear because the exact amount of CNTs transformed to TiC is unknown. However, the remained CNTs are expected to improve the mechanical properties which are consistent with the previous report [10, 13-15].

The microstructures of Ti composite materials after annealing are shown in **Fig. 6**(a)-(c). The microstructures show the presence of fine TiC particles and Ti matrix. TiC particles were possibly synthesized via reaction between Ti powder and CNTs during SPS process at 1073 K for 1.8 ks. This is because from a thermodynamic point of view, ΔG^o of TiC formation at 1073 K is -171.3 kJ/mol. [28], and the above reaction spontaneously progresses during the sintering process. TiC particles are distributed throughout the Ti matrix, which can account for the high dispersion of CNTs on the Ti powder surface during coating step. However, there are some large TiC particles existing in the microstructure. This is due to the clusters of individual CNTs at the facet or curve of Ti powder in **Fig. 1** are recombined and formed into a large TiC particle which is an inevitable phenomenon in the wet process. The *in-situ* formed TiC dispersoids both

before and after annealing almost show the same mean size of 2.0 μm as summarized in **Table 2**. The high distribution of TiC dispersoids effectively restrains the deformation of Ti grains which in turn maintain the stability of Ti grain during elevated temperature tensile testing. Moreover, the increase of TiC dispersoids is also effective to improve the retardation of Ti grain sliding. The microstructure observation of the tensile test sample of extruded Ti/TiCs composite by using 3.0wt.%CNTs/zwitterionic solution at the necking area confirms the retardation of grain boundary sliding by TiC particle as shown in **Fig. 6**(d)

The higher temperature causes the lower YS and TS of all tested samples. That can be explained by the diffusion-controlled creep phenomenon [29-31]. At elevated temperature, Ti atoms at grain boundaries which are parallel to the tensile stress axis can be diffused into another side of grain boundaries which are perpendicular to the tensile stress axis. It causes a plastic elongation of Ti grains along the tensile axis and decrease of the cross sectional area of the test specimen quickly. However, in the case of extruded Ti/TiCs composites containing a small mount of original CNTs, the YS and TS are higher than those of extruded pure Ti material. For example, the composite by using 3.0wt.%CNTs/zwitterionic solution shows YS and TS values higher than those of extruded pure Ti material of 40.4% and 109.1%, respectively, at the tested temperature of 673 K. This is because the *in-situ* formed TiC dispersoids inhibit the coarsening of Ti grain by their pining, as shown in the grain size measurement results at each testing temperature in **Fig. 6**(d) and **Table 2**, which in turn impede the motion of Ti atoms to another side of the grain boundaries. According to the quantitative analysis of TiC dispersoids from XRD results, the increase of TiC dispersoid content in the extruded Ti composites can effectively improve the retardation of Ti grain coarsening which in turn increases the stability of strength of the composites by the pinning and dispersion

strengthening mechanisms during elevated temperature tensile testing. Elongation of all extruded Ti/TiCs shows the lower percentage than that of extruded pure Ti material in every tested temperature. This is due to the fact that *in-situ* TiC dispersoid is a hard intermetallic phase which is never plastically deformed at elevated temperature of 673 K. As a result, the extruded Ti composite using 3.0wt.%CNTs/zwitterionic solution revealed the lowest elongation in all of the extruded Ti composite materials. The dependence of micro hardness on testing temperatures of the composites is shown in **Fig. 7**. The results indicate the decreasing tendency upon exposure at elevated temperature, and can be explained by the softening mechanism [32]. Dislocation and other defects of the composites are annihilated by the recovery process, resulting in decrease of the hardness of material. The rate of recovery is strongly dependent on temperature. Therefore, the micro hardness measurements of all samples at 573 K yield the lowest hardness value, compared to the other temperatures. The increase of TiC particles dispersed in the Ti matrix also helps to increase the resistance to the applied pressure during hardness test. Consequently, the extruded Ti composite by using 3.0 wt.% CNTs/zwitterionic solution can maintain higher hardness than those of 1.0 and 2.0 wt.% CNTs/zwitterionic samples, respectively.

In order to confirm the pinning effect of TiC dispersoids, the Ti composites were annealed at the higher temperatures of 573, 673 for 36 ks and 673 K for 360 ks. The evolution of microstructures is shown in **Fig. 8**. The microstructure of the extruded pure Ti material shows the increase of grain size when the annealing temperature is increased from 573 to 673 K, as shown in **Fig. 8** (a) and (b). On the other hand, the grain size measurement results of the composite materials show very small increase of Ti grain size as shown in successive **Fig. 8** (d)-(l). The small increase of Ti grain size can confirm the pinning effect of TiC dispersoids which help to suppress Ti grain growth during the

annealing process. The annealing at 673 K for 360 ks also shows very small changes in Ti grain size in the case of extruded Ti/TiCs composites. In contrast, the extruded pure Ti material shows the decrease in grain size, as shown in **Fig. 8** (c), because the recrystallization process occurs during long time annealing process according to the previous reports [20]. The presence of TiC dispersoids also retards the recrystallization of new grains when the long time annealing because the TiC pinning pressure is higher than driving pressure for recrystallization nucleation of new grain. Therefore, the recrystallization may never occurs in the case of the composites which are annealed at 673 for 360 ks as shown in **Fig. 8** (f), (i) and (l), respectively. High magnification images of extruded Ti/TiCs composites have also confirmed the unchanged Ti grain size after annealing at 673 K for 360 ks as shown in **Fig. 9**. The microstructural stability of the composites after annealing at different temperatures and times can be used to confirm the pinning effect due to TiC dispersoids which help to maintain the Ti grain size invariably during tensile testing at elevated temperatures.

4. Conclusions

1) The annealing process at 473 K for 360 ks significantly affected to the increase of grain size of extruded pure Ti material with no CNT.

2) the grain size of extruded Ti/TiCs composites never affected because the pinning effect of TiC dispersoids retarded the grain coarsening and stabilized the primary Ti grain size.

3) Mechanical properties at the elevated temperature of the composite materials indicated the decreasing tendency of tensile strength, yield strength and hardness.

4) The presence of TiC dispersoids in the Ti matrix effectively sustained the recovery process, resulting in maintaining stability of strength and hardness of the Ti composites during the elevated temperature.

References

1. S. Iijima, "Helical Microtubules of Graphitic Carbon", *Nature*, vol. 354 (1991) 56-58.

2. J.-P. Salvetat, J.-M. Bonard, N.H. Thomson, A. J. Kulik, L. Forró, W. Benoit, L. Zuppiroli, "Mechanical Properties of Carbon Nanotubes", *Applied Physics A*, 69 (1999) 255-260.

3. R. S. Ruoff and D. C. Lorents, "Mechanical and Thermal Properties of Carbon Nanotubes", *Carbon*, vol. 33, 7 (1995) 925-930.

4. S. R. Bakshi, D. Lahiri and A. Agarwal, "Carbon Nanotube Reinforced Metal Matrix Composites – A Review", *International Materials Reviews*, vol. 55, 1 (2010) 41-64.

5. R. George, K. T. Kashyap, R. Rahul and S. Yamdagni, "Strengthening in Carbon Nanotube/Aluminium (CNT/Al) Composites", *Scripta Materialia*, 53 (2005) 1159-1163.

6. A. M. K. Esawi and M. A. El Borady, "Carbon Nanotube-Reinforced Aluminium Strips", *Composites Science and Technology*, 68 (2008) 486-492.

7. L. Wang, H. Choi, J. M. Myoung and W. Lee, "Mechanical Alloying of Multi-Walled Carbon Nanotubes and Aluminium Powders for The Preparation of Carbon/Metal Composites", *Carbon*, vol. 47, 15 (2009) 3427-3433.

8. C. S. Goh, J. Wei, L. C. Lee and M. Gupta, "Simultaneous Enhancement in Strength and Ductility by Reinforcing Magnesium with Carbon Nanotubes", *Materials Science and Engineering A*, 423 (2006) 153-156.

9. C. S. Goh, J. Wei, L. C. Lee and M. Gupta, "Ductility Improvement and Fatigue Studies in Mg-CNT Nanocomposites", *Composites Science and Technology*, 68 (2008) 1432-1439.

10. K. Kondoh, H. Fukuda, J. Umeda, H. Imai, B. Fugetsu and M. Endo, "Microstructural and Mechanical Analysis of Carbon Nanotube Reinforced Magnesium Alloy Powder Composites", *Materials Science and Engineering A*, 527 (2010) 4103-4108.

11. P. Quang, Y. G. Jeong, S. C. Yoon, S. H. Hong and H. S. Kim, "Consolidation of 1 vol.% Carbon Nanotube Reinforced Metal Matrix Nanocomposites via Equal

Channel Angular Pressing", *Journal of Materials Processing Technology*, 187-188 (2007) 318-320.

12. W. M. Daoush, B. K. Lim, C. B. Mo, D. H. Nam and S. H. Hong, "Electrical and Mechanical Properties of Carbon Nanotube Reinforced Copper Nanocomposites Fabricated by Electroless Deposition Process", *Materials Science and Engineering A*, 513-514 (2009) 247-253.

13. K. Kondoh, T. Threrujirapapong, H. Imai, J. Umeda and B. Fugetsu, "CNTs/TiC Reinforced Titanium Matrix Nanocomposites via Powder Metallurgy and Its Microstructural and Mechanical properties", *Journal of Nanomaterials*, vol. 2008 (2008) Article ID127538, 4 pages, doi:10.1155/2008/127538

14. K. Kondoh, T. Threrujirapapong, H. Imai, J. Umeda and B. Fugetsu, "Characteristics of Powder Metallurgy Pure Titanium Matrix Composite Reinforced with Multi-Wall Carbon Nanotubes", *Composites Science and Technology*, 69 (2009) 1077-1081.

15. T. Threrujirapapong, K. Kondoh, H. Imai, J. Umeda and B. Fugetsu, "Hot Extrusion of Pure Titanium Reinforced with Carbon Nanotubes", *Steel Research International*, vol. 81, 9 (2010) 1320-1323.

16. F. Xue, S. Jiehe, F. Yan and C. Wei, "Preparation and Elevated temperature Compressive Properties of Multi-Walled Carbon Nanotube Reinforced Ti Composites", *Materials Science and Engineering A*, 527 (2010) 1586-1589.

17. C. Leyens and M. Peters, *Titanium and Titanium alloys*, Wiley-VCH, Germany (2003).

18. G. Lütjering and J.C. Williams, *Titanium*, 2nd ed., Springer-Verlag, Germany (2007).

19. B. D. Cullity and S.R Stock, *Elements of X-Ray Diffraction*, 3rd ed., Prentice Hall, USA, (2001).

20. F. J. Humphreys and M. Hatherly, *Recrystallization and Related Annealing Phenomena*, 2nd ed., Elsevier Ltd., Netherlands (2004)

21. H. Conrad, "Effect of Interstitial Solutes on The Strength and Ductility of Titanium", *Progress in Materials Science*, 26 (1981) 123-403

22. ASM Handbook vol. 3, *Alloy Phase Diagrams*, ASM International.

23. R. M. Aikin, Jr., "The Mechanical Properties of *In-Situ* Composites", JOM, 49, 8 (1997) 35-39.

24. Y. Kobayashi, Y. Tanaka, K. Matsuoka, K. Kinoshita, Y. Miyamoto and H. Murata, "Effect of Forging Ratio and Grain Size on Tensile and Fatigue Strength of Pure Titanium Forgings", *Journal of the Society of Materials Science*, Japan, vol. 54, 1 (2005) 66-72 (In Japanese).

25. M. E. Kassner and X. Li, "The Effect of Grain Size on The Elevated Temperature Yield Strength of Polycrystalline Aluminum", *Scripta Metallurgica et Materialia*, 25 (1991) 2833-2838.

26. C. Ouchi, H. Iizumi and S. Mitao, "Effects of Ultra-High Purification and Addition of Interstitial Elements on Properties of Pure Titanium and Titanium Alloy" *Materials Science and Engineering A*, 243 (1998) 186-195.

27. T. Threrujirapapong, T. Mimoto, K. Kondoh, J. Umeda and B. Fugetsu, "Effects of SPS Parameters on The Mechanical Properties and Microstructures of Titanium Reinforced with Multi-wall Carbon Nanotubes Produced by Hot Extrusion", *TMS 2011 140th Annual Meeting & Exhibition*, Supplemental Proceedings, vol. 2, (2011) 821-828, 27 February-3 March 2011, San Diego, California USA.

28. Y. H. Liang, H. Y. Wang, Y. F. Yang, Y. Y. Wang and Q. C. Jiang, "Evolution Process of The Synthesis of TiC in The Cu-Ti-C System", *Journal of Alloys and Compounds*, 452 (2008) 298-303.

29. W. F. Hosford, *Mechanical Behavior of Materials*, Cambridge University Press, UK (2005).

30. Y. Estrin, G. Gottstein, L. S. Shviddlerman, "Diffusion Controlled Creep in Nanocrystalline Materials under Grain Growth", *Scripta Materialia*, 50 (2004) 993-997.

31. M. J. R. Barboza, E. A. C. Perez, M. M. Medeiros, D. A. P. Reis, M. C. A. Nono, F. Piorino Neto and C. R. M. Silva, "Creep Behavior of Ti-6Al-4V and A Comparison with Titanium Matrix Composites", *Materials Science and Engineering A*, 428 (2006) 319-326.

32. B. Verlinde, J. Driver, I. Samajdar and R. D. Doherty, *Thermo-Mechanical Processing of Metallic Materials*, 1st ed., Pergamon, Netherlands (2007).

List of Tables

Table 1 Chemical compositions of the pure Ti powders (wt.%)

Materials	Purity	Fe	Cl	Mg	Si	N	C	O	Ti
Pure Ti	>95	0.03	<0.002	<0.001	0.01	0.02	<0.01	0.21	Bal.

Table 2 Average Ti grain size and TiC particle size before and after annealing at 473 K for 360 ks and after elevated temperature tensile testing at 473-673 K.

Size measurement	Extruded Ti	As-extruded	As-annealed	Tensile test temperature, K		
				473	573	673
Ti grain size, μm	Pure Ti	11.7	44.7	45.2	45.7	52.0
	1.0wt.%CNTs	8.6	8.4	8.4	8.5	10.3
	2.0wt.%CNTs	8.6	8.4	8.4	8.2	8.7
	3.0wt.%CNTs	7.4	7.7	7.4	7.7	7.7
TiC particle size, μm	1.0wt.%CNTs	2.0	2.1	2.2	2.2	2.1
	2.0wt.%CNTs	2.0	1.9	2.1	2.0	2.0
	3.0wt.%CNTs	2.1	2.0	2.1	1.9	2.1

Table 3 Lattice parameters of Ti matrix, TiC dispersoid amount, dissolved carbon atom in Ti matrix and the carbon content analysis of the extruded Ti/CNTs composites after annealing at 473 K for 3.6 ks.

Extruded materials	Lattice parameters, Å		TiC content, wt.%	Dissolved carbon atom, wt.%	Carbon content analysis, wt.%
	a axis	c axis			
Pure Ti	2.94473	4.67873	-	-	0.01
1.0wt.%CNTs	2.95243	4.69474	0.61	0.003385	0.27
2.0wt.%CNTs	2.95386	4.69698	1.58	0.003306	0.37
3.0wt.%CNTs	2.95156	4.69728	2.55	0.011661	0.76

* The maximum equilibrium solubility of carbon in α-Ti from is 0.4 wt.% [22]

Table 4 Incremental yield stress by grain size effect, carbon solid solution and TiC second phase of extruded Ti/CNTs composites at room temperature.

Extruded materials	Experimental yield stress, MPa	Incremental yield stress, MPa		
		Grain size	Carbon solid solution	Second phases (TiC + CNTs)
1.0wt.%CNTs	625	369	37	219
2.0wt.%CNTs	662	369	37	256
3.0wt.%CNTs	853	378	54	421
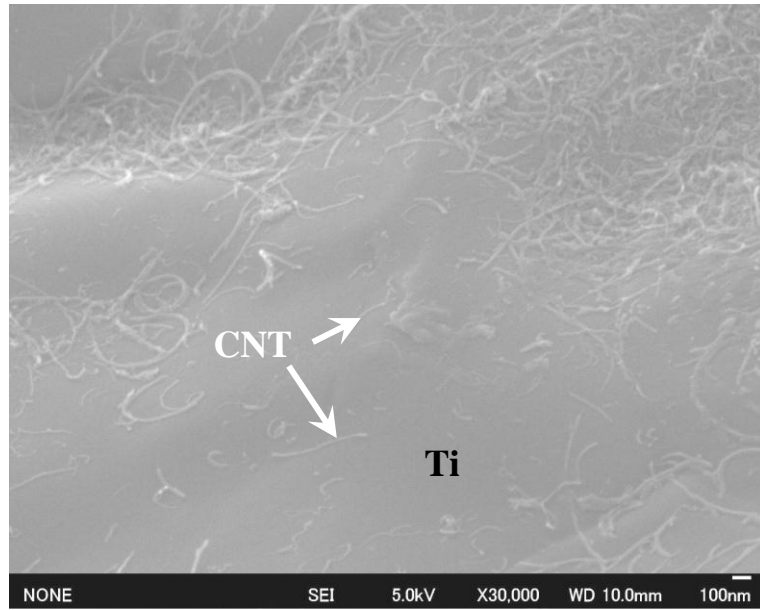
Fig. 1 High distribution of individual CNT on the Ti particle surface using 1.0wt.%CNTs/ zwitterionic solution

Fig. 2 Optical microstructures of the extruded pure Ti material without CNTs reinforcement (a) before and (b) after annealing at 473 K for 360 ks, compared to microstructure of the extruded pure Ti/CNT composite coated by 1.0wt.%CNTs/ zwitterionic solution (c) before and (d) after annealing at 473 K for 360 ks.
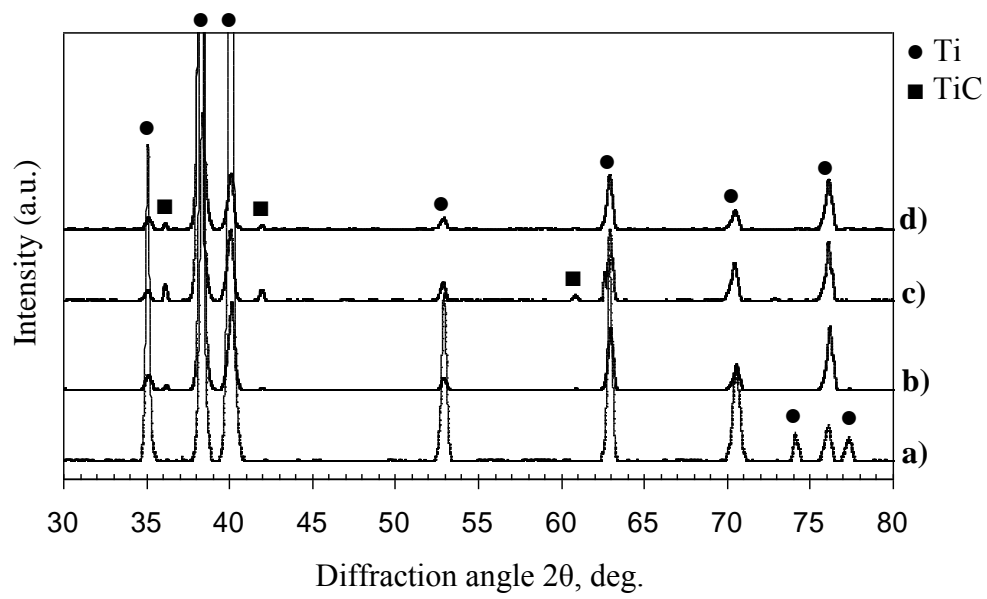
Fig. 3 XRD patterns of the extruded pure Ti composites after annealing at 473 K, (a) without reinforcement, (b) coated by 1.0, (c) 2.0 and (d) 3.0 wt.% CNTs/zwitterionic solution.
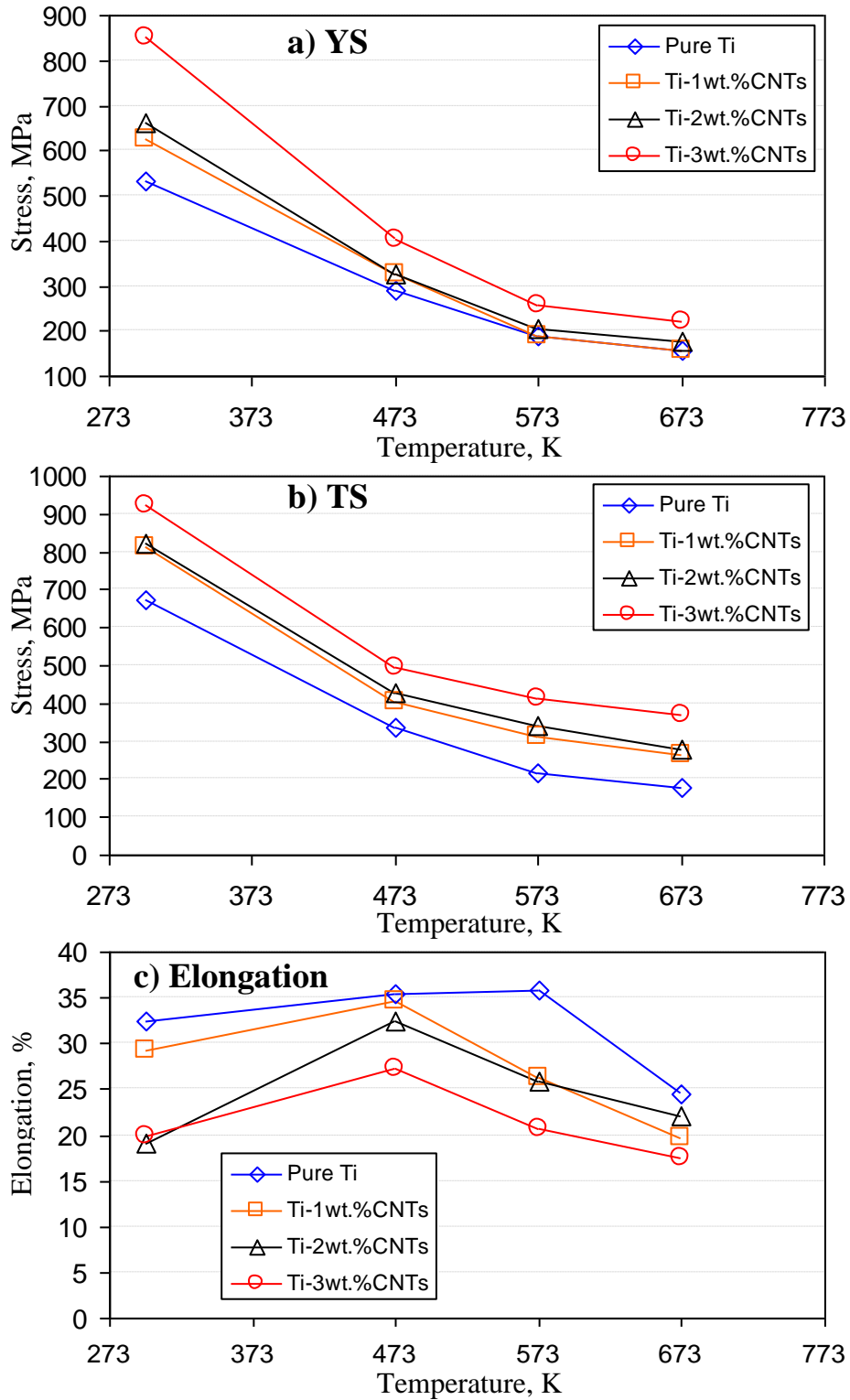
Fig. 4 Dependence of tensile properties on elevated temperatures of the extruded pure Ti composites coated by 1.0, 2.0 and 3.0 wt.% MWCNTs/zwitterionic solution; (a) yield stress, (b) tensile strength and (c) elongation.
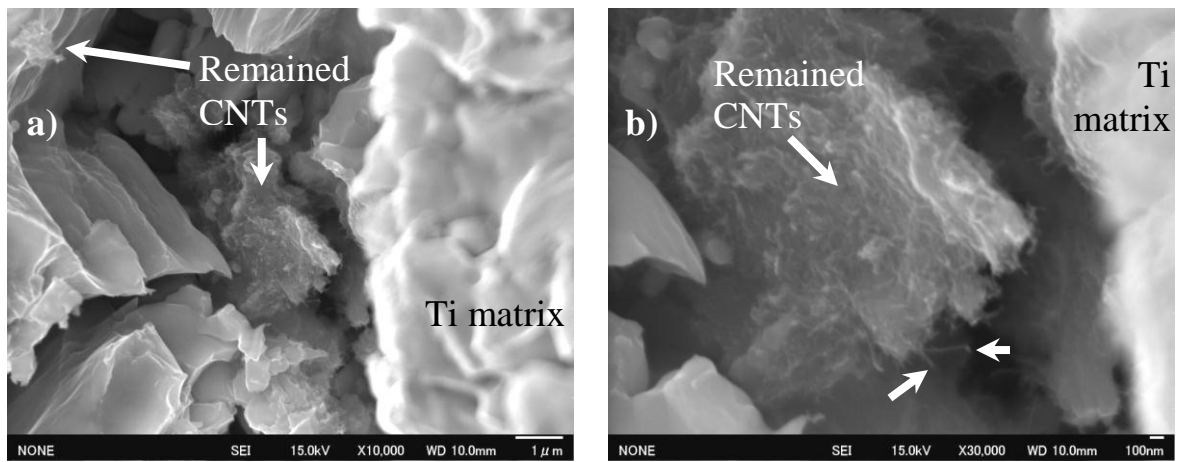
Fig. 5 SEM observation on fractured surface of the annealed sample of extruded pure Ti/CNTs coated by 1.0wt.% CNTs/zwitterionic solution after tensile testing at 673 K; (a) low magnification image, (b) high magnification image.
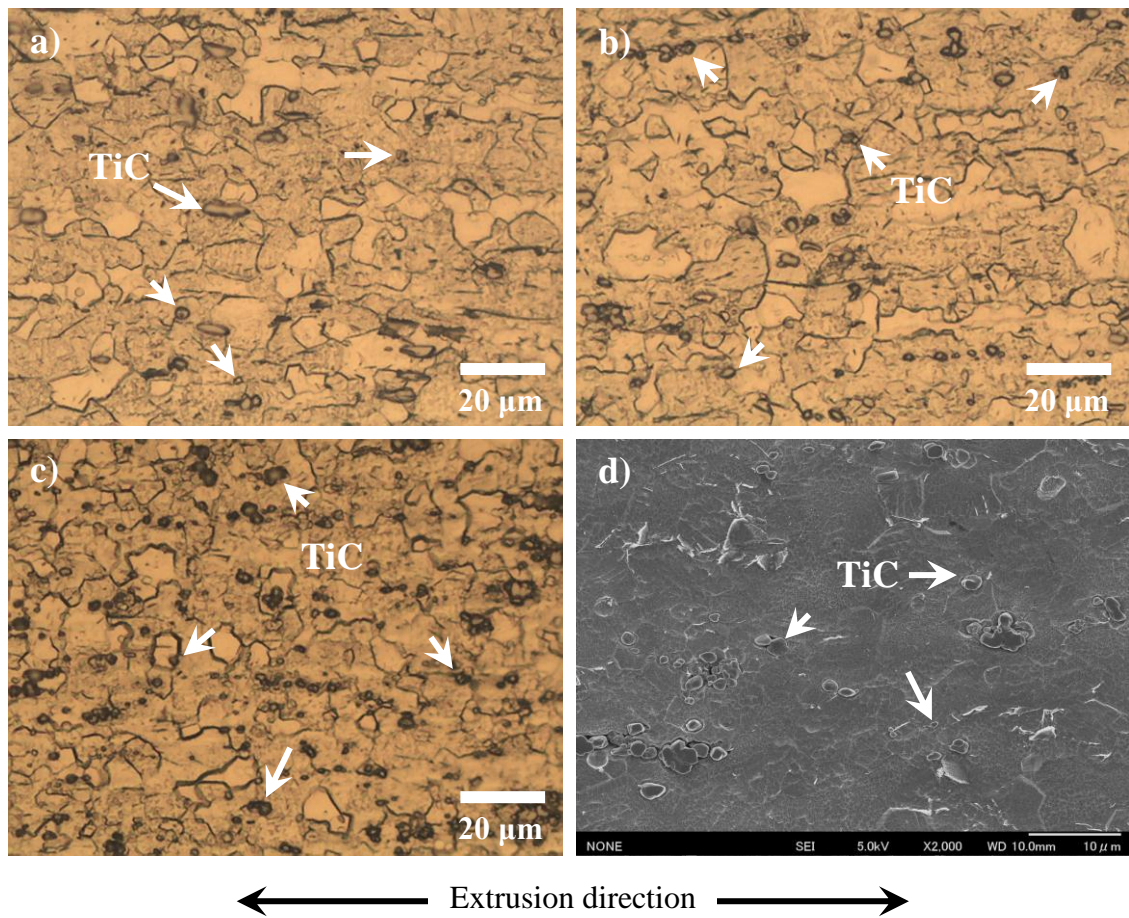
Fig. 6 Optical microstructures of the extruded pure Ti coated with (a) 1.0, (b) 2.0 and (c) 3.0 wt.% CNT/zwitterionic solutions after annealing at 473 K for 360 ks and (d) SEM microstructure at necking area of sample (c) after tensile testing at 673 K
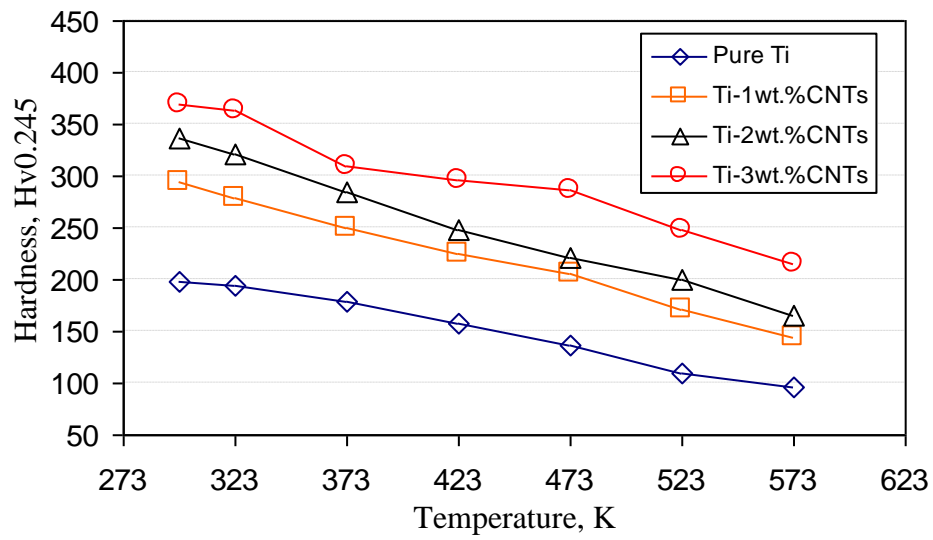
Fig. 7 Dependence of hardness on elevated temperatures of extruded pure Ti composites coated by 1.0, 2.0 and 3.0 wt.% CNTs/zwitterionic solution.
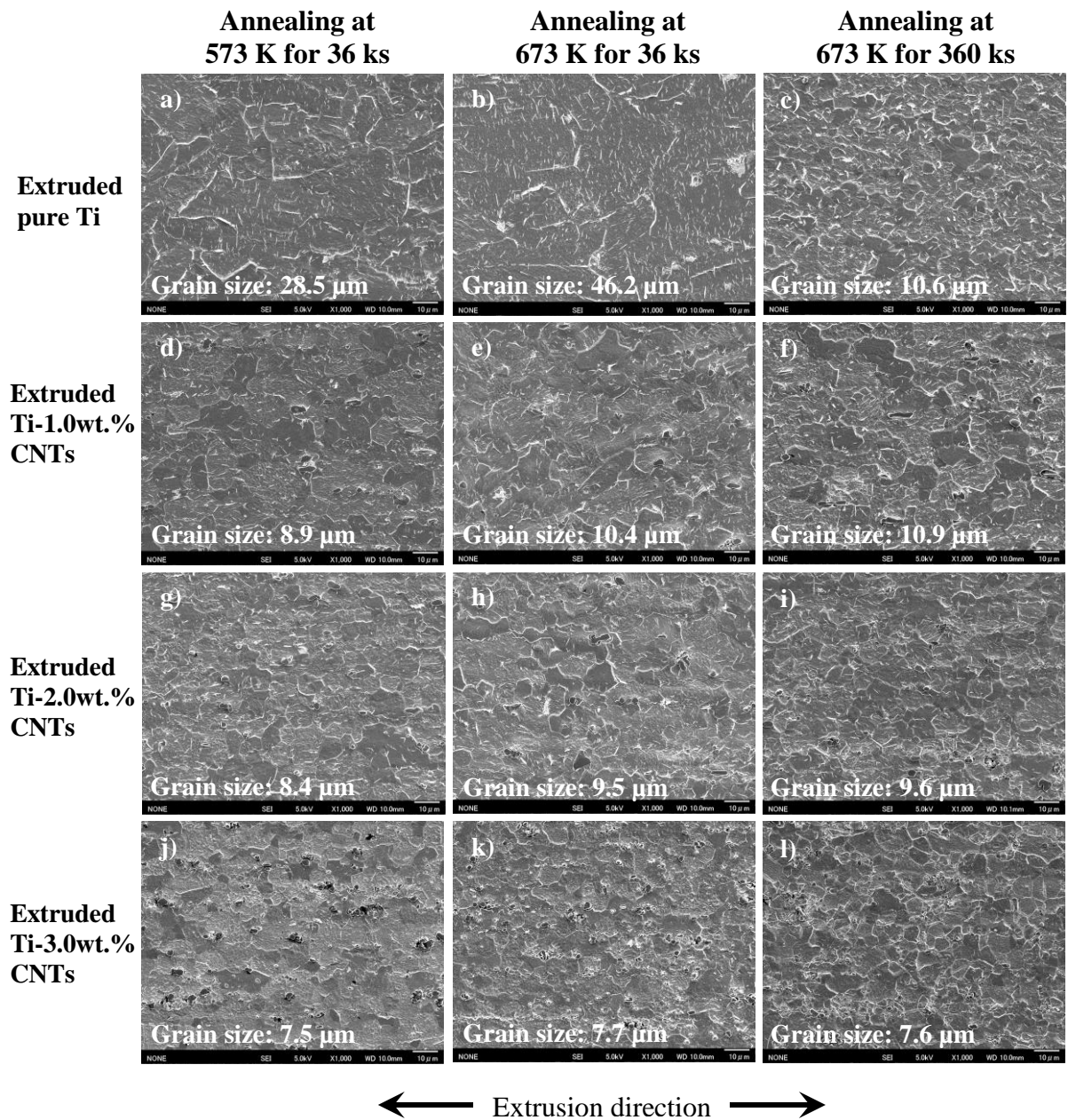
	Annealing at 573 K for 36 ks	Annealing at 673 K for 36 ks	Annealing at 673 K for 360 ks
Extruded pure Ti	a) Grain size: 28.5 μm	b) Grain size: 46.2 μm	c) Grain size: 10.6 μm
Extruded Ti-1.0wt.% CNTs	d) Grain size: 8.9 μm	e) Grain size: 10.4 μm	f) Grain size: 10.9 μm
Extruded Ti-2.0wt.% CNTs	g) Grain size: 8.4 μm	h) Grain size: 9.5 μm	i) Grain size: 9.6 μm
Extruded Ti-3.0wt.% CNTs	j) Grain size: 7.5 μm	k) Grain size: 7.7 μm	l) Grain size: 7.6 μm

← Extrusion direction →

Fig. 8 Microstructure of extruded Ti/CNTs composites after annealing at 573 and 673 K for 36 ks and 673 K for 360 ks.
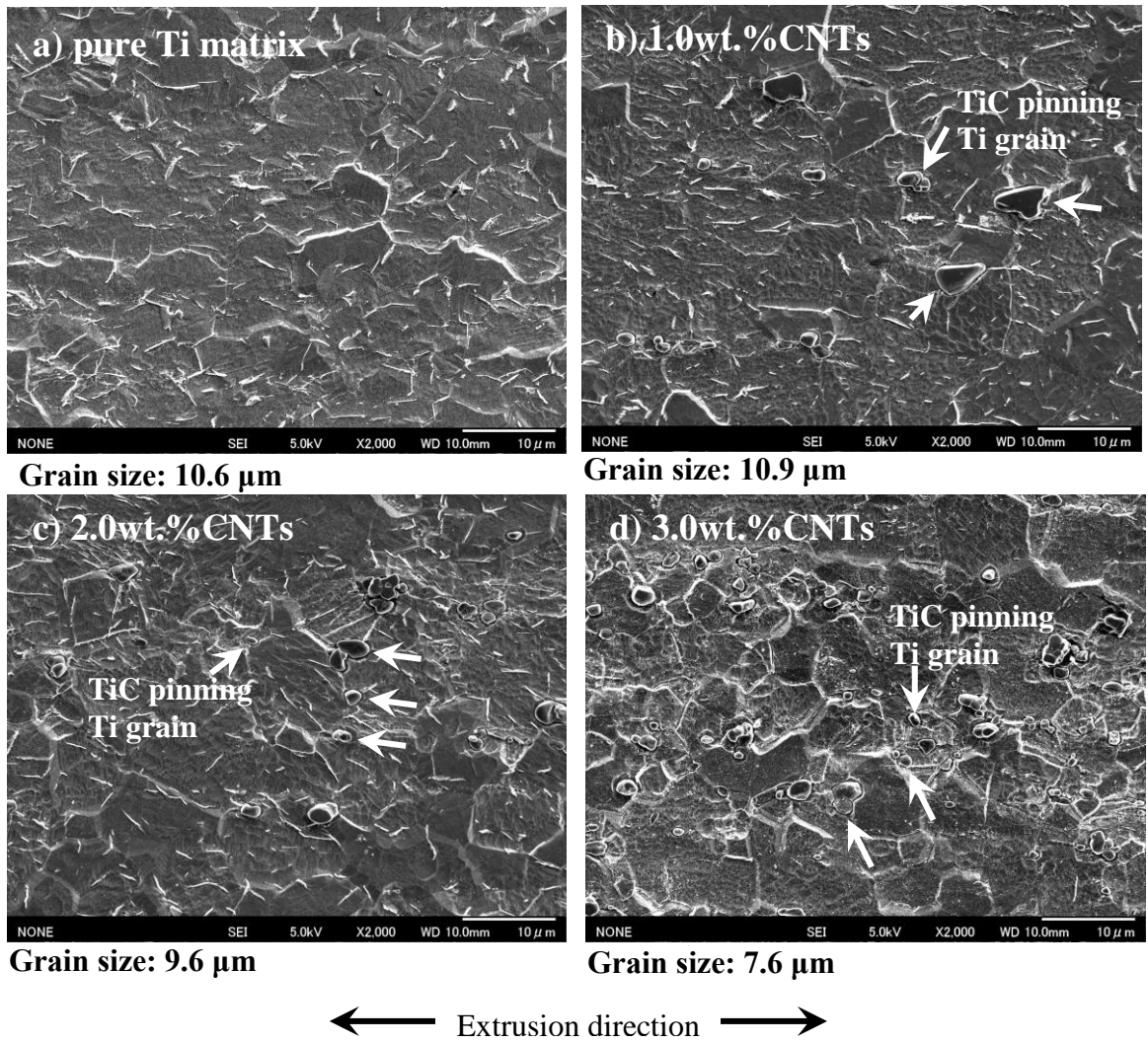
Fig. 9 SEM images of (a) recrystallized grain of extruded pure Ti material and unchanged Ti grain size due to TiC pinning effect of the samples coated by (b) 1.0wt.%, (c) 2.0wt.% and (d) 3.0 wt.% CNTs/zwitterionic solution after annealing at 673 K for 360 ks.